and hexadecane (HD) provide useful measures of wettability. Since the pure methyl-terminated monolayer is hydrophobic ($\theta_a(H_2O) = 114°$, $\theta_a(HD) = 48°$), and the alcohol-terminated monolayer is hydrophilic ($\theta_a(H_2O) = \theta_a(HD) \approx 0°$), contact angles are very sensitive to the composition of the monolayer and the structure of the surface.

Figure 2 plots the ellipsometric thickness, contact angles of water and hexadecane, and XPS peak areas of gold and oxygen against R.[11] Here we note two salient features of these graphs: a detailed discussion will be deferred to a subsequent paper. First, ellipsometry and XPS peak areas indicate a dramatic change in the composition of the monolayer over a narrow range of solution composition, $R = 7-20$. This change in the composition of the monolayer is closely correlated with a sharp increase in the hydrophilicity and oleophilicity of the surface as measured by the advancing contact angles of water and hexadecane, respectively.[12] Thus the structure of the surface on a microscopic scale is clearly and directly linked to the wettability of the monolayer, an important macroscopic quantity. Second, the inflection in the curves occurs, not at $R = 1$, but at $R \approx 11$.[13,14] This difference between solution and surface compositions is a general feature of competitive adsorption experiments.[15] In this experiment, van der Waals forces between close-packed hydrocarbon chains favor adsorption of the longer chain thiol.

We attempted to model the composition of the monolayer by a simple equilibrium expression (eq 1) between the solution and the surface (dotted curve in Figure 2, upper graph) where the

$$HSC_{10}CH_2OH_{surface} + HSC_{21}CH_{3solution} \rightleftharpoons HSC_{10}CH_2OH_{solution} + HSC_{21}CH_{3surface} \quad (1)$$

equilibrium constant $K_{eq} = 11$, *independent* of solution concentration. Clearly the observed data do not follow this simple expression: the two components of the monolayer do not act independently and may act cooperatively to minimize the free energy. Monolayers composed predominantly of the long-chain methyl-terminated thiol $HSC_{21}CH_3$ (maximizing the chain-packing interactions) or the short-chain hydroxy-terminated thiol $HSC_{10}CH_2OH$ (maximizing H-bonding both with the solvent and within the monolayer) are preferred over monolayers containing a mixture of the thiols.[16] The data do not, however, take the form of step functions in R, which would be expected thermodynamically if the formation of macroscopic islands were favored.[17] Over a narrow range of R it is possible to form intermediate monolayers containing both thiols; the exact structure of these monolayers is not clear, but the data are consistent with a model in which the two components segregate into small clusters on the surface. These monolayers provide a model system for studying the wettability of complex structures and for examining how polar groups interact to minimize their energy in a nonpolar environment.[18]

Mixed monolayers of thiols on gold allow us to engineer ordered, two-dimensional systems with Å-level control over thickness and structure and with chemical control over wettability. Synthetic variation of the tail groups and chain lengths provides great flexibility in the design of the interfacial structures and gives these systems wide applicability in the physical, biological, and medical sciences.

Acknowledgment. We are grateful to R. Nuzzo and M. Wrighton for helpful discussions.

Registry No. $HS(CH_2)_{11}OH$, 73768-94-2; $HS(CH_2)_{21}CH_3$, 7773-83-3; Au, 7440-57-5.

(11) We prefer log R to the mole fraction, χ, as the abscissa because $kT \log R$ is related to the Gibbs free energy, and hence this choice of axis highlights thermodynamic contributions to the adsorption process.

(12) Hexadecane and water interact predominantly by dispersion and polar forces, respectively. The detailed inferences from the contact angle data and comparisons with other monolayer systems will be discussed in a subsequent paper.

(13) The ellipsometric thickness yields a value of $R(\chi_{1/2}) = 11$ where $\chi_{1/2}$ = 1:1 ratio of the two thiols in the monolayer. XPS peak areas yield $R(\chi_{1/2})$ = 10–12 depending on the model used to analyze the data.

(14) The monolayer system had not quite reached equilibrium when these measurements were made. Over a period of 2 weeks $R(\chi_{1/2})$ slowly increased to $R \approx 14$.

(15) Bain, C. D.; Whitesides, G. M., unpublished results.

(16) Despite being enthalpically disfavored, some $HSC_{21}CH_3$ is incorporated into the $HSC_{10}CH_2OH$ monolayer even at large R (and vice versa) due to the favorable entropy of mixing.

(17) We believe that absorption of thiols onto gold is controlled to a large extent by thermodynamics, although kinetics also play a role, as evinced by the slow change in the monolayer composition with time after the initial, rapid absorption.

(18) Israelachvili, J. N. *Intermolecular and Surface Forces*; Academic: New York, 1985.

Novel Triple Cubane-Type Organometallic Oxide Clusters: $[MCp^*MoO_4]_4 \cdot nH_2O$ (M = Rh and Ir; Cp* = C_5Me_5; n = 2 for Rh and 0 for Ir)

Yoshihito Hayashi, Koshiro Toriumi,* and Kiyoshi Isobe*

Institute for Molecular Science
Myodaiji, Okazaki 444, Japan

Received December 8, 1987

In recent years there has been a growing interest in the metal oxide clusters containing organometallic groups and polyoxoanions, a field which has been developed by W. G. Klemperer, W. Knoth, and R. G. Finke.[1] These novel clusters provide models for metal oxide surfaces which are catalysts for a variety of hydrocarbon transformations, and they represent a meeting point for the chemistry of low-valent and high-valent transition metals. This communication reports structures and properties of newly prepared organometallic oxide clusters possessing a novel triple cubane framework.

Aqueous solution (5 cm^3, pH 7.3) of $Na_2MoO_4 \cdot 2H_2O$ (2.0 g, 8.3×10^{-3} mol) was added dropwise to a suspension of (partially dissolved) $[RhCp^*Cl_2]_2$ (0.5 g, 8.0×10^{-4} mol) in water (3 cm^3, pH ca. 3.8), and the mixture was stirred at 25 °C for 3 h to deposit a yellow-orange solid. In the case of $[IrCp^*Cl_2]_2$, a yellow solid was obtained after refluxing at 100 °C for 1 h. These products were recrystallized from CH_2Cl_2–C_6H_5Me (1:1 by volume) with 93% and 68% yields for Rh (red crystals) and Ir (yellow crystals) complexes, respectively. Both new complexes gave satisfactory analyses and molecular weights for the molecular formula $[M(C_5Me_5)MoO_4]_4 \cdot nH_2O$ (n = 2 for M = Rh (**1**) and 0 for Ir (**2**)); and the water of crystallization is easily lost under vacuum at room temperature.[3] These complexes are soluble in most organic solvents except hydrocarbons. The rhodium complex is also slightly soluble in water and shows a molar conductivity of 75.9 S cm^2 mol^{-1} (concentration of complex: 4.35×10^{-4} mol dm^{-3}) at 25 °C. X-ray photoelectron spectra of **1** and **2** show the oxidation states of the Mo, Rh, and Ir atoms to be +6, +3, and +3, respectively (binding energies, Mo 3d5/2: 231.4 (for **1**), 231.3 eV (for **2**); Rh 3d5/2: 308.8 eV; Ir 4f7/2: 61.7 eV).[4]

(1) (a) Day, V. W.; Klemperer, W. G. *Science (Washington, D.C.)* **1985**, *228*, 533–541. (b) Domaille, P. J.; Knoth, W. H. *Inorg. Chem.* **1983**, *22*, 818–822. (c) Finke, R. G.; Rapko, B.; Domaille, P. J. *Organometallics* **1986**, *5*, 175–178. (d) Muetterties, E. L. *Chem. Eng. News: Special Report* **1982**, Aug. 30, pp 28–41. (e) Pope, M. T. "Heteropoly and Isopoly Oxometalates" In *Inorganic Chemistry Concepts No. 8*; Springer-Verlag: Berlin, Heidelberg, New York, Tokyo, 1983; pp 118–127.

(2) Kang, J. W.; Moseley, K.; Maitlis, P. M. *J. Am. Chem. Soc.* **1969**, *91*, 5970–5977.

(3) **1**: Anal. Calcd for $C_{40}H_{64}Mo_4O_{18}Rh_4$ (dihydrate): C, 29.51; H, 3.96. Found: C, 30.17; H, 3.80; mol wt calcd for anhydrous **1** 1592, found 1480. **2**: Anal. Calcd for $C_{40}H_{60}Ir_4Mo_4O_{16}$: C, 24.64; H, 3.10. Found: C, 24.56; H, 3.11; mol wt calcd 1949, found 1860. The molecular weights were determined by vapor pressure osmometry in dichloromethane at 27 °C.

(4) The corresponding values of binding energy in the starting materials, $Na_2Mo^{VI}O_4 \cdot 2H_2O$ (Mo 3d5/2, 231.5 eV), $[Rh^{III}Cp^*Cl_2]_2$ (Rh 3d5/2, 308.3 eV), and $[Ir^{III}Cp^*Cl_2]_2$ (Ir 4f7/2, 61.3 eV) are very close to those in **1** and **2**. Observed values were corrected by assuming C_{1s} binding energy in Cp* rings of **1** and **2** as 284.6 eV.

0002-7863/88/1510-3666$01.50/0

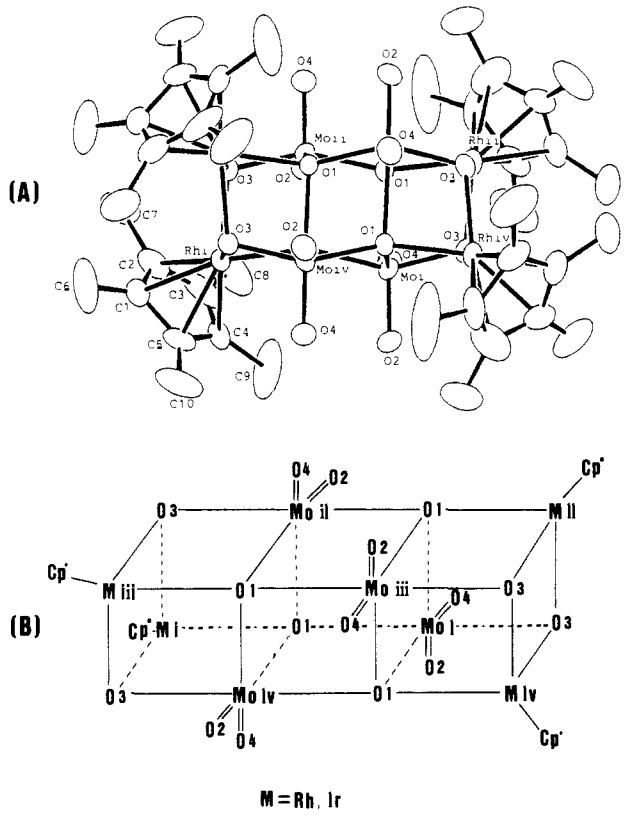

Figure 1. Molecular structure of the oxide cluster $[RhCp^*MoO_4]_4$ (**1**): (A) ORTEP diagram and (B) simplified drawing with the numbering scheme.[8] Important bond lengths (Å) and angles (deg) (the values for **2** are given in brackets) not mentioned in the text are as follows: M(i)–O(1)(i), 2.098 (8), [2.09 (2)]; M(i)–O(3)(ii), 2.133 (8), [2.16 (2)]; M(i)–O(3)(iv), 2.132 (8), [2.11 (2)]; Mo(i)–O(1)(i), 1.967 (8), [1.96 (2)]; Mo(i)–O(1)(ii), 2.338 (7), [2.33 (2)]; Mo(i)–O(1)(iv), 2.341 (8), [2.37 (2)]; Mo(i)–O(3)(i), 1.901 (8), [1.89 (2)]; Mo(i)–O(2)(i), 1.697 (8), [1.72 (2)]; Mo(i)–O(4)(i), 1.712 (8), [1.70 (2)]; M(i)···M(iii), 3.332 (2), [3.361 (3)]; M(i)···Mo(ii), 3.220 (1), [3.256 (3)]; M(i)···Mo(iv), 3.230 (1), [3.257 (3)]; Mo(i)···Mo(ii), 3.359 (2), [3.343 (5)]; O(1)(i)–M(i)–O(3)(ii), 78.1 (3), [76.6 (6)]; O(1)(i)–M(i)–O(3)(iv), 77.8 (3), [75.8 (7)]; O(3)(ii)–M(i)–O(3)(iv), 76.5 (3), [74.7 (6)]; O(1)(i)–Mo(i)–O(3)(i), 143.5 (3), [142.0 (6)]; O(1)(ii)–Mo(i)–O(1)(iv), 68.9 (3), [69.0 (6)]; Mo(ii)–O(1)(i)–Mo(iv), 110.9 (3), [111.0 (7)]; M(ii)–O(3)(i)–M(iv), 102.7 (3), [103.8 (9)]; Mo(i)–O(3)(i)–M(iv), 105.8 (4), [106.9 (7)]; Mo(i)–O(3)(i)–M(ii), 106.3 (4), [109.1 (8)].

X-ray structure analyses[5] of **1** and **2** revealed that the crystals are isomorphous and that they contain a novel triple cubane framework consisting of two $M_2Mo_2O_8$ (M = Rh, Ir) cores. The molecules have S_4 crystallographic symmetry as shown in Figure 1 for **1**.[6] Important bond distances and angles are given in the caption to Figure 1. The central cube consists of four molybdenum and four oxygen atoms which occupy alternate vertices. Each Mo atom is surrounded by two terminal and four bridging oxygen atoms to form a distorted octahedron. The bridging O(1) atoms have a remarkably distorted tetrahedral geometry (Rh(i)–O(1)(i)–Mo(i)[8] = 152.7 (4)°, Ir(i)–O(1)(i)–Mo(i) = 152.3 (9)°). In general the Mo–O bond length will become larger with an increasing number of metal atoms bound to an oxygen atom. Thus the mean Mo–O(terminal), Mo–O(M_2), and Mo–O(Mo_2M) distances are 1.705 (8, 8, 8, 2)[9], 1.901 (8), and 2.215 (8, 166, 248, 3) Å for **1** and 1.71 (2, 1, 1, 2), 1.89 (2), and 2.22 (2, 17, 26, 3) Å for **2**, respectively. The bond angles of the MoO_2 fragments in **1** and **2** (104.7 (4) and 107.0 (8)°, respectively) are close to the value in $[Mo_7O_{24}]^{6-}$.[10] The external cubes are made up of $M_2Mo_2O_4$ (M = Rh, Ir). The M atoms have a distorted octahedral geometry and achieve 18-electron configurations by binding three adjacent bridging O atoms (two O(3) and one O(1)) and a Cp* ring. This bridging mode has been observed previously for $[RhCp^*(cis\text{-}Nb_2W_4O_{19})]^{2-}$.[11] The M···M, M···Mo, and Mo···Mo distances indicate no bonding interaction between the respective metal atoms. The water molecule in **1** is linked by hydrogen bonds to two terminal oxygen atoms (O(2)(i) and O(4)(iv)).

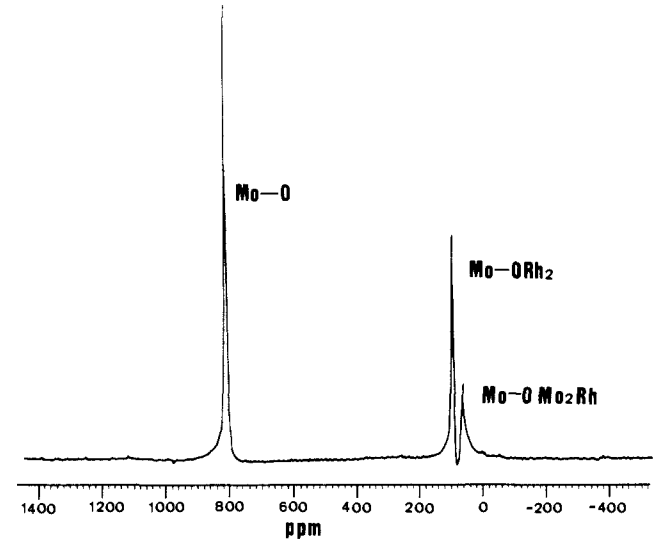

Figure 2. ^{17}O NMR spectrum of anhydrous $[RhCp^*MoO_4]_4$ in $CDCl_3$.

In accordance with isomorphous compounds, **1** and **2** exhibit quite similar IR spectra in the 400–1000-cm^{-1} region, three Mo=O(terminal) stretching bands in the 890–930-cm^{-1} region, and four Mo–O(bridging) vibration bands in the 500–700-cm^{-1} region.[12]

Samples of **1** and **2** enriched in ^{17}O have been prepared in ^{17}O-enriched water, with which $[MoO_4]^{2-}$ readily exchanges at pH ca. 7. They display three completely resolved ^{17}O NMR signals as shown in Figure 2 for **1**.[13] These are easily assigned to chemically nonequivalent oxygen atoms on the basis of the previously established qualitative correlation between the upfield shift and the increasing number of metal atoms to which an oxygen

(5) Crystal data are as follows: **1**, cubic, space group $I\bar{4}3d$, a = 25.285 (2) Å, Z = 12, D_x = 2.01 g cm^{-3}; **2**, cubic, space group $I\bar{4}3d$, a = 25.141 (4) Å, Z = 12, D_x = 2.45 g cm^{-3}. Intensity data were collected on a Rigaku AFC-5 diffractometer with graphite-monochromated Mo Kα radiation in the $2\theta \leq 60°$ range. The structures were solved by a direct method (MULTAN 78) and refined by a full-matrix least-squares technique. The current R values of **1** and **2** are 0.037 for 1237 and 0.057 for 1152 independent absorption-corrected reflections, respectively.

(6) Half the molecular structure of **1** and **2**, consisting of M(ii), O(3)(i), O(1)(ii), Mo(i), Mo(ii), O(1)(i), O(3)(ii), and M(i) atoms, corresponds to the structure of $[(C_5H_4Me)_2Mo_2O_4]_2$.[7] Clearly, the Cp*M (M = Rh, Ir) and the $(C_5H_4Me)_2Mo$ groups differ in coordination number and size. Thus the former group can offer three coordination sites forming the vertex of a cube, whereas the latter has only two sites, and thus can only occupy the corner of a square plane. In addition, two C_5H_4Me rings in the latter group are too bulky to construct a cube. These factors may explain the preference for the triple-cubane structure in our system.

(7) Prout, K.; Daran, J.-C. *Acta Crystallogr., Sect. B; Struct. Crystallogr. Cryst. Chem.* **1978**, *B34*, 3586–3591.

(8) (a) The Roman numerals, shown only for the metals, stand for the numbering scheme of symmetry operation. (b) Identical atoms with the same Arabic numerals are related to one another by an S_4 symmetry operation. Arabic numerals of the M and Mo atoms and the Cp* groups are omitted for clarity.

(9) The numbers in parentheses are written according to Klemperer's method. The first, second, and third numbers are the average of the standard deviations, the average and maximum deviations from the averaged value of bond lengths, respectively. The fourth number represents the number of data. See ref 11 also.

(10) Evans, H. T. jun.; Gatehouse, B. M.; Leverett, P. *J. Chem. Soc., Dalton Trans.* **1975**, 505–514.

(11) Besecker, C. J.; Day, V. W.; Klemperer, W. G.; Thompson, M. R. *J. Am. Chem. Soc.* **1984**, *106*, 4125–4136.

(12) IR spectra of **1** and **2**: Mo=O(terminal) stretching region **1**; 922 (s), 896 (s), and 886 cm^{-1} (sh); **2**, 932 (s), 908 (s), and 896 cm^{-1} (sh); Mo–O(bridging) vibration region **1**, 692 (s), 644 (s), 578 (s), and 536 cm^{-1} (s); **2**, 694 (s), 644 (s), 580 (s), and 536 cm^{-1} (s).

(13) ^{17}O NMR chemical shifts, referenced to D_2O at 25 °C (lower field positive) **1**, δ 846 (OMo), 144 (OMoRh$_2$), and 112 (OMo$_3$Rh); **2**, δ 867 (OMo), 133 (OMoIr$_2$), and 120 (OMo$_3$Ir). The intensity ratio of these signals is 2:1:1 in both clusters.

atom is bonded.[14] This order of the chemical shift is also consistent with the trend in Mo–O bond lengths.[15] The ^{95}Mo and ^{103}Rh nuclei in the clusters are separately equivalent in $CDCl_3$ (^{95}Mo NMR, δ 176 for **1**, 191 for **2**; ^{103}Rh NMR, δ 4079 for **1**).[16] The ^{1}H and ^{13}C NMR spectra indicate that all four Cp* rings in both clusters are magnetically equivalent.[17] These NMR data confirm that the triple cubane structure is preserved in $CDCl_3$.

The oxygen atoms in the clusters do not exchange with H_2O in $CDCl_3$. Clusters **1** and **2** in solid decompose only at high temperatures such as 275 and 290 °C, respectively, indicating that the triple cubane structure is very stable. Reaction of $[WO_4]^{2-}$ with $[RhCp^*Cl_2]_2$ gave a similar cluster $[RhCp^*WO_4]_4$, and its properties are now under investigation.

Acknowledgment. We thank Professors Shinichi Kawaguchi of Kinki University and Martin A. Bennett (a visiting professor of IMS) for valuable discussions.

Supplementary Material Available: ORTEP diagram of **2**, listings of fractional coordinates with equivalent isotropic thermal parameters, anisotropic thermal parameters, bond distances, and bond angles for **1** and **2** (7 pages); listings of observed and calculated structure factors for **1** and **2** (15 pages). Ordering information is given on any current masthead page.

(14) Filowitz, M.; Klemperer, W. G.; Messerle, L.; Shum, W. *J. Am. Chem. Soc.* **1976**, *98*, 2345–2346.
(15) Che, T. M.; Day, V. W.; Francesconi, L. C.; Fredrich, M. F.; Klemperer, W. G. *Inorg. Chem.* **1985**, *24*, 4055–4062.
(16) The ^{95}Mo and ^{103}Rh NMR chemical shifts were referenced to 1 M Na_2MoO_4 in D_2O at 25 °C and Ξ(^{103}Rh) of 3.16 MHz, respectively (lower field positive).
(17) ^{1}H NMR ($CDCl_3$) C_5Me_5 δ 1.75 s (for **1**), 1.67 s (for **2**); ^{13}C NMR ($CDCl_3$) C_5Me_5 δ 9.33 s (for **1**), 9.60 s (for **2**); C_5Me_5 δ 90.15 d (for **1**, J_{C-Rh} = 8.8 Hz), 81.35 s (for **2**).

The "Gilman Reagent" Ph_2CuLi and "Higher Order" Ph_3CuLi_2: ^{13}C and ^{6}Li NMR in Dimethyl Sulfide[1]

Steven H. Bertz* and Gary Dabbagh

AT&T Bell Laboratories
Murray Hill, New Jersey 07974
Received December 21, 1987

Higher order organocuprates[2a] have recently joined the classical Gilman reagents[2b] at the forefront of synthetic methodology. While "Me_3CuLi_2" had been postulated as a reactive intermediate, Lipshutz et al. showed by means of ^{1}H and ^{7}Li NMR that the addition of MeLi to Me_2CuLi does not form a higher order species, i.e., the reagent is merely Me_2CuLi + MeLi.[4] In contrast, to within the limits of NMR detection, free MeLi is not present in the higher order cyanocuprate $Me_2Cu(CN)Li_2$,[5] the stability of which has been attributed to dπ-backbonding.[6] On the basis of chemical reactivity, House et al. conjectured the existence of "Ph_3CuLi_2";[7] however, this reagent has not been confirmed spectroscopically. We find that Ph_3CuLi_2 in dimethyl sulfide (DMS)[8] is a novel, identifiable reagent. When prepared from CuI in DMS, Ph_2CuLi exists primarily as a halide-containing cluster. By using CuBr, we obtain halide-free Ph_2CuLi.

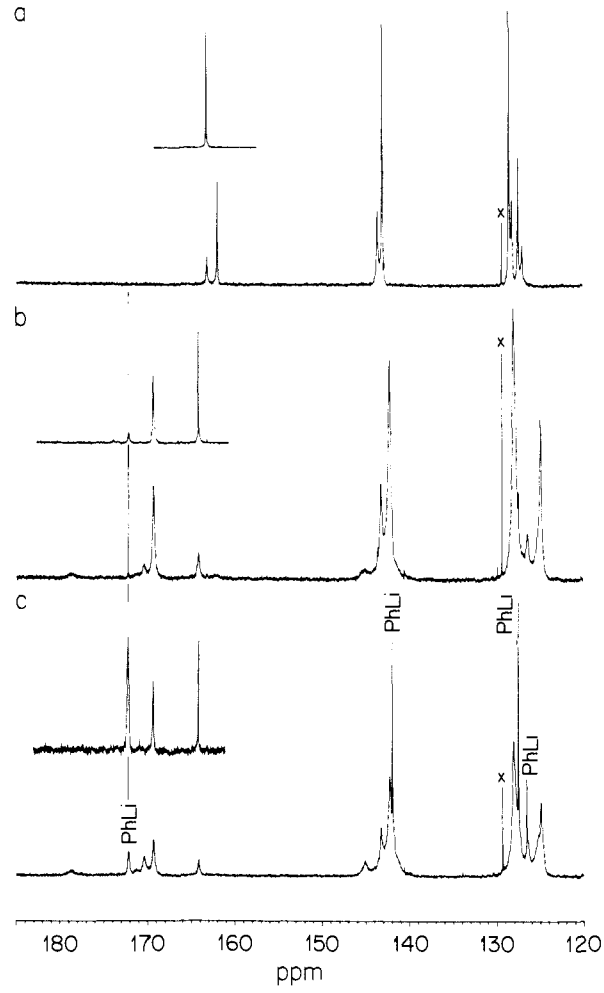

Figure 1. ^{13}C NMR spectra (173 K) of (a) Ph_2CuLi, (b) Ph_3CuLi_2, and (c) Ph_3CuLi_2 + PhLi prepared from CuI in DMS (10% $C_6{}^2H_{12}$ for internal lock). Benzene (δ 129.3) is indicated by X. The scale places $C_6{}^2H_{12}$ at δ 26.4 ppm. Insets are for reagents prepared from CuBr.

At −100 °C in DMS, the ^{13}C NMR spectrum (Figure 1a) of Ph_2Cu^6Li, prepared from CuI and 2 equiv of Ph^6Li,[9a] consists of eight lines: four major (δ 161.9, ipso; 143.0, ortho; 128.5, meta; 127.4, para)[9b] and four minor (163.1, 143.6, 128.1, 127.0 ppm), due to two kinds of Ph groups. The two sets coalesce to one set of four lines at ca. −80 °C (δ 162.1, 143.1, 128.3, 127.2, see Figure 3, Supplementary Material). By substituting CuBr for CuI, "halide-free" Ph_2CuLi is obtained, owing to the precipitation of LiBr from DMS. The four peaks in the ^{13}C NMR spectrum of this material are at precisely the same positions as the peaks of the minor Ph_2CuLi species from CuI (e.g., see Figure 1a, inset). Thus, as far as the iodocuprate is concerned, the major species at low temperature (70% by integration of the ^{13}C NMR spectrum) contains LiI.

The ^{6}Li NMR spectra of Ph_2CuLi prepared from CuI and from CuBr (Figure 2a) are in harmony with the ^{13}C NMR results. The

(1) Part 14 in the series New Copper Chemistry. Part 13: Bertz, S. H.; Gibson, C. P.; Dabbagh, G. *Organometallics* **1988**, *7*, 227. Part 12: ref 16a.
(2) (a) Lipshutz, B. H.; Wilhelm, R. S.; Kozlowski, J. A. *Tetrahedron* **1984**, *40*, 5005. (b) Posner, G. H. *An Introduction to Synthesis Using Organocopper Reagents*; Wiley: New York, 1980.
(3) Macdonald, T. L.; Still, W. C. *J. Am. Chem. Soc.* **1975**, *97*, 5280.
(4) Lipshutz, B. H.; Kozlowski, J. A.; Breneman, C. M. *J. Am. Chem. Soc.* **1985**, *107*, 3197. This paper appears to obviate the earlier report of the ^{1}H NMR spectrum of "Me_3CuLi_2" by Ashby and Watkins (Ashby, E. C.; Watkins, J. J. *J. Am. Chem. Soc.* **1977**, *99*, 5312).
(5) Lipshutz, B. H.; Kozlowski, J. A.; Wilhelm, R. S. *J. Org. Chem.* **1984**, *49*, 3943.
(6) Lipshutz, B. H.; Kozlowski, J. A.; Wilhelm, R. S. *J. Org. Chem.* **1983**, *48*, 546.
(7) House, H. O.; Koepsell, D. G.; Campbell, W. J. *J. Org. Chem.* **1972**, *37*, 1003.
(8) For the preparation of organocuprates in DMS, see: Clark, R. D.; Heathcock, C. H. *Tetrahedron Lett.* **1974**, 1713. House, H. O.; Chu, C.-Y.; Wilkins, J. M.; Umen, M. J. *J. Org. Chem.* **1975**, *40*, 1460.
(9) (a) Ph^6Li was prepared by the method of Schlosser and Ladenberger (Schlosser, M.; Ladenberger, V. *J. Organomet. Chem.* **1967**, *8*, 193). All Li used was ^{6}Li unless otherwise specified. The organocopper reagents were prepared by adding a cold (≤0 °C) solution of PhLi in DMS to a cold solution of CuI in DMS in a 10-mm NMR tube and bringing the resulting solution (~0.2 M) to 0 °C before cooling it in the probe of a Bruker AM360. Ca. 10% [$^2H_{12}$]cyclohexane was included for the internal ^{2}H lock. (b) The assignment of the ^{13}C NMR spectrum is based on an analysis of the coupling constants $J_{CCH} \approx 0$ and $J_{CCCH} \approx 6$ Hz. The same order is observed for PhLi (see ref 13).

0002-7863/88/1510-3668$01.50/0